International Symposium on Experimental Robotics
ISER '99

Experimental Validation of Physics-Based Planning and Control Algorithms for Planetary Robotic Rovers

Karl Iagnemma Robert Burn Eric Wilhelm Steven Dubowsky
Department of Mechanical Engineering
Massachusetts Institute of Technology
Cambridge, MA 02139 U.S.A.
dubowsky@mit.edu

Abstract: Robotic planetary exploration is a major component of the United States' NASA space science program. The focus of our research is to develop rover planning and control algorithms for high-performance robotic planetary explorers based on the physics of these systems. Experimental evaluation is essential to ensure that unmodeled effects do not degrade algorithm performance. To perform this evaluation a low-cost rover test-bed has been developed. It consists of a rocker-bogie type rover with an on-board manipulator operating in a rough-terrain environment. In this paper the design and fabrication of an experimental rover system is described, and the experimental validation of several rover control algorithms is presented. The experimental results obtained are key to the evaluation and validation of our research.

1. Introduction

On July 4, 1997, the Mars Pathfinder mission landed the Sojourner telerobotic rover on the surface of Mars [1]. The United States' NASA plans planetary robotic missions in the years 2001, 2003, and 2005 to Mars with far more ambitious performance objectives than those set for Sojourner. Future planetary explorers will need to navigate rugged terrain and travel substantial distances, while exercising a high degree of autonomy [2,3]. The focus of our research at the MIT Mechanical Engineering Field and Space Robotics Laboratory (FSRL) is on developing methods and algorithms for the design, planning and control of high-performance robotic planetary explorers based on the physics of these systems.

To validate the effectiveness of the developed algorithms, experimental evaluation is essential. To perform this evaluation a low-cost rover test-bed has been developed (see Figure 1). The FSRL rover is a 6-wheeled rocker-bogie vehicle that is similar kinematically to the JPL Lightweight Survivable Rover (LSR) (see Figure 2) [4]. The FSRL rover has a three degree-of-freedom manipulator mounted on the front of its chassis. It uses several prototype end-effector concepts for manipulation of rock samples. The experimental system chassis contains shape memory alloy

(SMA) actuated variable geometry mechanisms that re-configure the system to improve its ability to traverse difficult terrain. All power is provided by on-board batteries. Low-level control and planning are performed using an on-board PC/104 computing architecture. A wireless modem is used for external communication to obtain high-level commands from a task planner. The experimental system weighs 6.1 kg. and was constructed for less than $10,000.

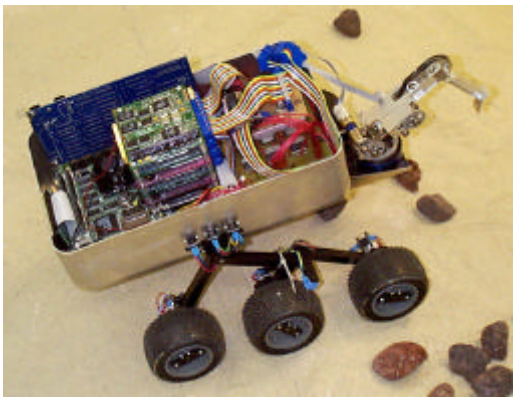

Figure 1: The Field and Space Robotics Laboratory (FSRL) Rover (without cover)

In our research, algorithms have been developed that use rover models which are designed to be practical for on-board implementation. Based of these models, a fuzzy logic traction control algorithm has been developed [5,6]. Rough terrain path-planning algorithms have also been developed [5,7]. Finally, a high-performance manipulator control algorithm developed for fixed-base manipulators has been successfully extended to the rover-mounted manipulator case [8]. To demonstrate the effectiveness of these algorithms with the FSRL rover, an 8' by 10' laboratory terrain has been constructed with challenging Mars-like features, such as hills, rocks, and an extended ditch system.

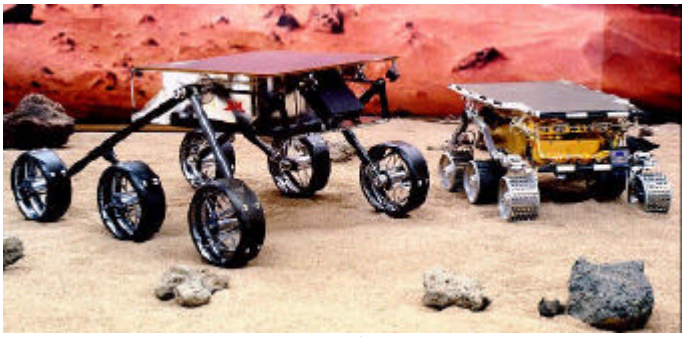

Figure 2: The JPL LSR (left) and Sojourner (right)

2. Rover Mechanical Design

The rover mechanical system is based on a six-wheeled rocker-bogie design, which is widely utilized by NASA due to its excellent mobility characteristics (see Figure 3) [9]. The rover features six independently powered wheels driven by geared Portescap DC motors. A 501:1 gear reduction produces a peak output torque of 100

oz-in and maximum angular velocity of 12 rpm. The resulting maximum velocity of the rover is approximately 8 cm/sec. The rover is steered with skid-steering. The suspension of the rover is constructed from aluminum square tubing, and includes integral motor mounts. The body is made from a formed aluminum sheet and supports the system electronics and sensors. The body also serves as an attachment point for a manipulator arm and stereo cameras. A mechanical differential allows the body to "split the difference" of the two rocker angles. The total cost of construction of the mechanical structure was approximately $2500.

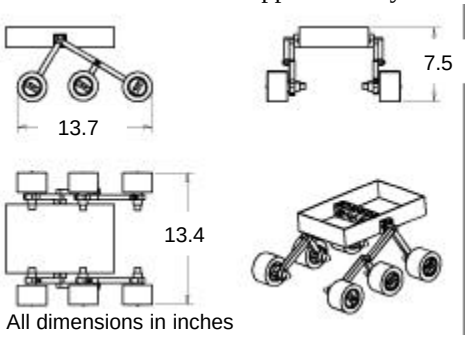

Figure 3: Experimental Rover Dimensions

2.1. Manipulator

The three degree-of-freedom manipulator mounted on the front of the rover is shown in Figure 4. The manipulator's light weight (approximately 16 ounces) is achieved by using low-weight aluminum members and small, highly geared motors. The joints are driven by MicroMo DC motors with gear ratios of 2961:1, 3092:1, and 944:1 at the trunk, shoulder, and elbow joints, respectively. With the high gear reduction, the manipulator is capable of exerting large forces. In some configurations, it can exert a force equal to one-half the rover weight. This high-force capability could be useful for manipulator-aided mobility or trap recovery. The base of the arm is mounted to a six degree-of-freedom force-torque sensor, which is used for control (see Section 4.1) [8].

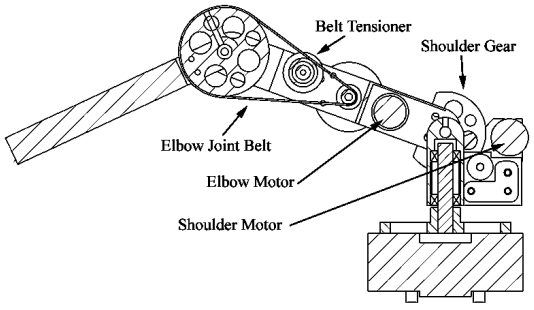

Figure 4: Three Degree-of-Freedom Manipulator

2.1.1. End-Effector

Several end-effector concepts have been developed for handling rock samples. The most effective has proven to be a lightweight three-fingered end-effector. It utilizes

flexural joints and relies on shape-memory alloy (SMA) actuation (see Figure 5). Each of the three fingers are formed from 1/8" steel rod. A nylon mounting plate has integral flexures that allow motion without bearing surfaces, eliminating the need for lubrication and considerably simplifying design and fabrication. A 0.006" diameter Flexinol SMA wire provides retracting force to each finger from its normally closed position. The wires are connected to the ends of the fingers, and run along the bottom of the mounting plate to increase their working length, and thus allow greater finger travel.

The three-fingered gripper is designed to be able to grasp rocks up to 2 ½" in diameter, and be able to support the weight of a typical volcanic-type rock of that size. The prototype end-effector weighs 2 ounces.

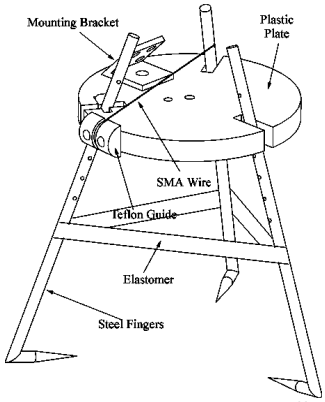

Figure 5: Three-Fingered End-Effector

2.2. Reconfigurability

An SMA-actuated reconfigurable rocker-bogie suspension concept has been developed which allows the rover to modify its geometry to improve mobility and avoid failure situations. The mechanism allows the rover to squat one or both sides of its suspension, and thus increase its stability margin when required (for example, when the rover is on a transverse slope). Additionally, reconfigurability allows the rover to reposition its center of mass when performing traction control [5,6].

An illustration of a reconfigurable rocker mechanism is shown in Figure 6. A Flexinol SMA wire provides retracting force for the rocker, and a multi-jaw coupling locks the rocker links in place, fixing the rocker angle. The SMA wire is routed over Delrin wire guides to increase the working length.

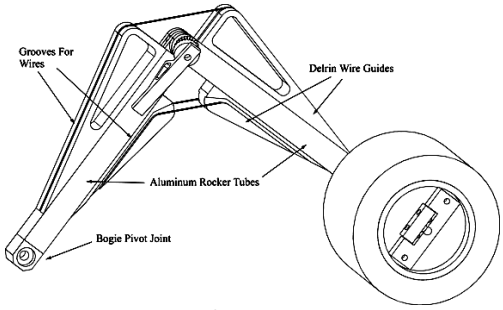

Figure 6: Reconfigurable Rocker Concept

3. Electronic and Power System

The rover electronics system was designed to be compact, low-cost and lightweight (see Figure 7). A block diagram of the system can be seen in Figure 8. The system is based on a PC/104 486 computing platform, with additional modules for digital and analog IO, encoder reading, and interface to a JR3 six-axis force/torque sensor which is mounted underneath the manipulator (see Section 2.1). NiCad rechargeable batteries power the rover. The rover is outfitted with a full suite of sensors including motor tachometers and encoders, rocker/bogie angle potentiometers, and a three-axis accelerometer. Communication with an operator is accomplished via a National Semiconductor AirShare wireless modem operating at 9600 baud. The total cost of the electronic system was less than $6000.

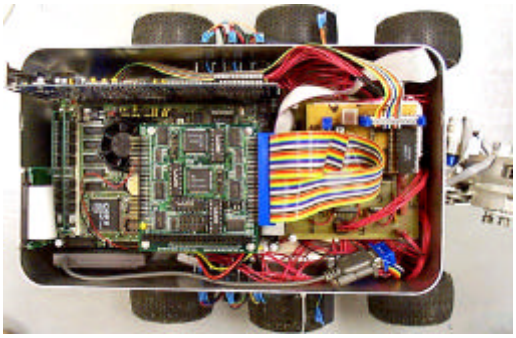

Figure 7: Rover Electronics Packaging

3.1. Computation

Computation is performed on a 486DX2 66 Mhz PC/104 single-board computer. A PC/104 computing platform was chosen due to its small size, light weight, and low power consumption [10]. The motherboard is 203 mm by 146 mm, with a functional depth of 40 mm, and weighs 15.5 ounces. It operates on a single power supply of 5 volts at 2 amps. It is interfaced via the PC/104 bus to modules which perform A/D conversion, D/A conversion, and digital input and output.

The system can support 8 differential A/D channels, 16 single-ended A/D channels, 16 D/A channels, 80 digital IO lines, and 8 quadrature encoders. It can also power 12 motors via pulse-width modulation.

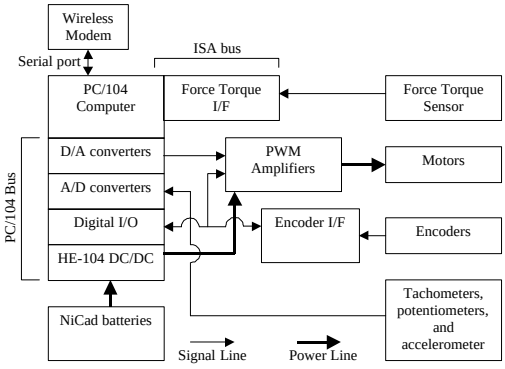

Figure 8: Electronic System Block Diagram

3.2. Power

The rover is powered by NiCad batteries. Each battery pack is rated at 7.2 volts and has a capacity of 1700 mAh, and the rover uses two battery packs connected in series. A Tri-M Engineering Systems PC/104 HE-104 DC/DC converter provides power to the system. The DC/DC converter can provide 50 watts of continuous filtered power, and is very tolerant of shocks and vibration. Motor control of the drive motors and manipulator motors is accomplished through PWM amplifiers.

3.3. Sensing

The rover is equipped with numerous sensors to monitor its performance and determine its state. The six drive wheels are equipped with tachometers, which are read by differential A/D lines. The three manipulator motors are equipped with magnetic encoders, and are read by a custom interface based on a US Digital LS7266R1 dual quadrature encoder chip. A three-axis Crossbow CXL04M3 accelerometer is mounted on the body of the rover, to determine its roll and pitch relative to an inertial frame. A JR3 67M25A six-axis force/torque sensor is mounted under the base of the manipulator. A dedicated ISA bus board provides interface support for the force/torque sensor. Finally, potentiometers are mounted on the rocker and bogie joints to determine their angular position.

4. Rover Analysis and Control

The Field and Space Robotics Laboratory has been actively researching control algorithms for planetary rovers in recent years. Recently, a high-performance manipulator control algorithm developed for fixed-base manipulators has been successfully extended to the rover-mounted manipulator case [8]. A fuzzy logic traction control algorithm has been developed [5,6]. Rough terrain path-planning algorithms have also been developed [5,7].

Two of these algorithms are described briefly in the following subsections. Experimental results using the rover testbed are presented in Section 5.

4.1. Rover-Mounted BSC Control

Planetary rover-mounted manipulators are expected to perform high-precision tasks such as instrument placement. These lightweight manipulators have large gear ratios, which leads to high drivetrain friction and makes high-precision control difficult. A control algorithm called Base-Sensor Control (BSC) has been developed for high-precision control of fixed-base manipulators with high joint friction [8]. This method utilizes feedback from a six-axis force/torque sensor mounted under the base of the manipulator, which is used to estimate the torque at each manipulator joint. With an estimate of the joint torque, accurate joint torque control is possible and disturbances such as friction can be rejected. This leads to improved friction compensation, which in turn improves the execution of fine-motion tasks.

4.1.1. BSC Control Overview

A simplified version of the BSC control algorithm has been developed for slow manipulator motions such as might be required in planetary scientific tasks [8]. This simplified algorithm relies only on feedback from the force/torque sensor and

knowledge of the manipulator configuration and kinematic parameters. In this simplified algorithm, the torque at a manipulator's n joints is estimated as:

$$t = \mathbf{A}(q)\left(\mathbf{W}_{\text{base}} - \mathbf{Y}(q)f\right) \quad (1)$$

where **A**(q) is an nx6 matrix that depends on the manipulator joint configurations and kinematic parameters, $\mathbf{W}_{\text{base}}$ is a 6x1 vector containing the wrench measured by the force/torque sensor, **Y**(q) is a 6xm matrix that relies on the manipulator joint configurations, and f is an mx1 vector of manipulator mass parameters. Note that the quantity $(\mathbf{Y}(q)\cdot f)$ represents gravity compensation.

The estimated joint torque is used in a control scheme comprised of an inner torque-control loop and an outer position-control loop (see Figure 9). An inner loop integral compensator provides low-pass filtering and zero steady-state error. A simple proportional-derivative controller is employed in the outer loop. This simple control architecture has been shown to provide very precise position control during small, slow motions [8].

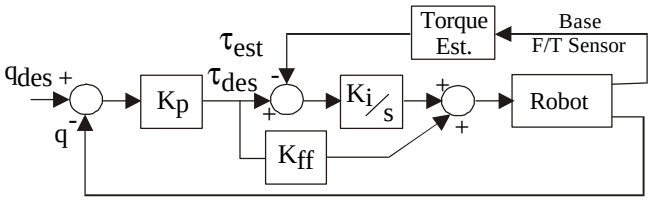

Figure 9: BSC Control Block Diagram

4.1.2. Rover-Mounted BSC Control

The above control algorithm can be modified for application to rover-mounted manipulators by assuming that the motion of the rover is slow enough that dynamic forces applied to the force/torque sensor by rover motion are negligible. Then Equation 1 becomes:

$$t = \mathbf{A}(q)\left(\mathbf{W}_{\text{base}} - \mathbf{Y}(q,\Psi,\Theta)f\right) \quad (2)$$

The gravity compensation matrix **Y** is now a function of both the manipulator configuration and the rover body pitch (Ψ) and roll (Θ). Note also that manipulator mass parameters which previously did not appear in f (i.e. were "unidentifiable") may now appear uniquely [11].

Equation (2) is used to estimate the joint torque of a rover-mounted manipulator, and a control scheme identical to that shown in Figure 9 can be implemented. Current work in the Field and Space Robotics Laboratory involves extending this control method to allow for rover dynamic effects.

4.2. Rough-Terrain Traction Control

Future planetary exploration missions will require rovers to traverse challenging terrain in order to achieve scientific objectives. Traction control reduces unplanned wheel slip, and thus improves traversability in rough terrain. Traction control also improves localization accuracy, and reduces power consumption.

An analysis of a planar rocker-bogie type rover has been performed with the goal of developing a traction control system [6]. It shows that the force balance equations of the system shown in Figure 10 can be written in the form:

$$\mathbf{M} \cdot \begin{bmatrix} F_x^i \\ N_1 \\ N_2 \\ N_3 \end{bmatrix} = \mathbf{X} \tag{3}$$

where **M** is a 4x4 matrix of ground contact angles and kinematic parameters, and **X** is a 4x1 vector of the rover kinematics and the input (traction) forces T_1, T_2, and T_3. The system is solvable by inverting **M**, either analytically or numerically.

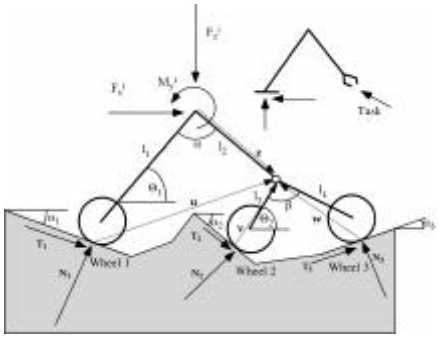

Figure 10: Traction Control Force Analysis

From this analysis, a control scheme could be developed for on-line optimal traction control. However, this requires knowledge of wheel-ground contact angles, which are difficult to measure in practice. To circumvent this problem, a set of heuristic rules have been developed based on the preceding analysis [6]. Based on these heuristics, a fuzzy-logic controller has been developed that systematically exploits the heuristics. The controller utilizes the desired wheel angular velocity, the measured angular velocities of the wheels, and an estimate of the slip at each wheel.

5. Experimental Results

The control methods described above have been tested on the FSRL rover operating in our Mars-like laboratory terrain.

5.1. Rover-Mounted BSC Control Results

Figures 11a and 11b show typical experimental results of the rover-mounted BSC algorithm compared with standard PID control. Here, the first and second (torso and shoulder) joints of the manipulator were commanded to track 0.2º amplitude 0.05 hz sinusoids. At these very slow speeds, nonlinear friction effects can dominate manipulator tracking performance. The tracking performance of joints one and two have been plotted against one another for compactness. The BSC-controlled manipulator had an RMS error of 0.0138º, compared to 0.0297º for PID control. The maximum error was reduced from 0.0749º for PID control to 0.0322º for BSC.

Essentially, BSC control reduced the position errors of the manipulator by approximately 50%, a substantial performance improvement. This improvement was difficult to predict with simulation due to system compliance and complex backlash in the rover differential. Experimentation showed that BSC control is robust to these unmodeled phenomena.

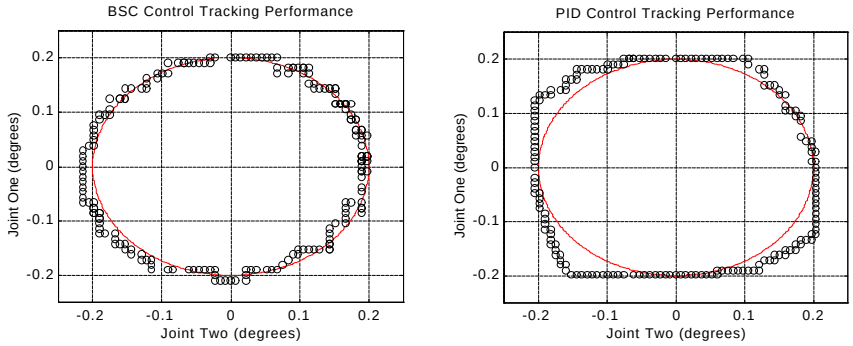

(a) *(b)*

Figure 11: BSC Tracking Performance (Figure 11a) vs. PID (Figure 11b)

5.2. Rough-Terrain Traction Control Results

For experimental evaluation of the fuzzy-logic control algorithm the rover was commanded to perform slope and step climbing tasks under various loading conditions. In the slope climbing task the rover was commanded to traverse a slope with a grade of approximately 18 degrees, which created a near-slip situation. In the step climbing task the rover was commanded to traverse a sharp step followed by a slope. Results of the success rate of the fuzzy logic controller is summarized in Table I and compared to conventional PI velocity control.

Table I: Summary of Results of Slope and Step Climbing Tasks

	Fuzzy Logic	PI Velocity Control
Slope Task	85%	60%
Step Task	63%	27%

The fuzzy logic controller performed better than the PI controller in the slope climbing task, where it improved the success rate by 42%. The fuzzy logic controller significantly improved performance in the step climbing task, where it improved the success rate by 133%. Current work in the Field and Space Robotics Laboratory involves refining the heuristics of the fuzzy logic controller, and improving the slip-detection algorithm. These factors should further improve the performance of the fuzzy logic controller.

6. Conclusions

A low-cost rover test-bed has been developed, which consists of a rocker-bogie type rover with an on-board manipulator operating in a rough-terrain environment. It has a three degree-of-freedom manipulator mounted on the front of the rover chassis, which uses a prototype end-effector for manipulation of rock samples. The experimental system chassis contains shape memory alloy (SMA) actuated variable

geometry mechanisms that re-configure the system to improve its ability to traverse difficult terrain. Power is provided by on-board batteries, and control is performed using an on-board PC 104 computing architecture.

The rover has proven very useful in the study of advanced control algorithms for planetary robotic explorers. Examples of experimental validation of a high-performance rover-mounted manipulator control algorithm and a fuzzy logic traction control algorithm have been presented.

7. Acknowledgements

This work is supported by the NASA Jet Propulsion Laboratory under contract number 960456. The authors would like to acknowledge the support of Dr. Paul Schenker and Dr. Eric Baumgartner at JPL. The support and encouragement of Guillermo Rodriguez is also acknowledged.

8. References

[1] Golombek, M. P. 1998 Mars Pathfinder Mission and Science Results. In: *Proceedings of the 29th Lunar and Planetary Science Conference*

[2] Matijevic, J., 1997 01 Surveyor Rover: Requirements, Constraints and Challenges (www.cs.cmu.edu/~meteorite/2001rover/)

[3] Hayati, S., Volpe, R., Backes, P., Balaram, J., and Welch, W. 1996 Microrover Research for Exploration of Mars. In: *AIAA Forum on Advanced. Developments in Space Robotics*

[4] Schenker, P., Sword, L., Ganino, et al. 1997 Lightweight Rovers for Mars Science Exploration and Sample Return. in: *Proceedings of SPIE XVI Intelligent Robots and Computer Vision Conference*

[5] Farritor, S., Hacot, H., and Dubowsky, S. 1998 Physics-Based Planning for Planetary Exploration. In: *1998 IEEE International Conference on Robotics and Automation*

[6] Hacot, H. 1998 *Analysis and Traction Control of a Rocker-Bogie Planetary Rover.* M.S. Thesis, Massachusetts Institute of Technology

[7] Iagnemma, K., Genot, F. and Dubowsky, S. 1999 Rapid Physics-Based Rough-Terrain Rover Planning with Sensor and Control Uncertainty. In: *1999 IEEE International Conference on Robotics and Automation*

[8] Morel, G., Iagnemma, K., and Dubowsky, S. The Precise Control of Manipulators with High Joint Friction Using Base Force/Torque Sensing. Submitted to *Automatica: The Journal of the International Federation of Automatic Control*

[9] Bickler, D. 1992 The New Family of JPL Planetary Surface Vehicles. In: Proceedings of the International Symposium On Missions, Technologies, and Design of Planetary Mobile Vehicles

[10] Wilhelm, E. 1998 *Design of a Wireless Control System for a Laboratory Planetary Rover.* B.S. Thesis, Massachusetts Institute of Technology

[11] West, H., Papadopoulos, E., Dubowsky, S., and Cheah, H. 1989 A Method For Estimating the Mass Properties of a Manipulator by Measuring the Reaction Moments at its Base. In: *IEEE International Conference on Robotics and Automation*